

International Journal of Modern Physics: Conference Series
 © World Scientific Publishing Company

Charmonium and light hadron spectroscopy

Chengping Shen

*School of Physics and Nuclear Energy Engineering, Beihang University
 Beijing, 100191, China
 shencp@ihep.ac.cn*

In this report I review some results on the charmonium and light hadron spectroscopy mainly from BESIII and Belle experiments. For the charmonium, the contents include the observation of $\psi(4040)/\psi(4160) \rightarrow \eta J/\psi$, the measurements of the $\eta_c/\eta_c(2S)$ resonance parameters and their decays, the evidence of the $\psi_2(1^3D_2)$ state in the $\chi_{c1}\gamma$ mass spectrum. For the light hadron spectroscopy, the contents include the $X(1835)$ research in $e^+e^- \rightarrow J/\psi + X(1835)$ and $\gamma\gamma \rightarrow \eta'\pi^+\pi^-$ processes, and the analysis of the $\eta\eta$, $\omega\phi$, $\phi\phi$ and $\omega\omega$ mass spectra in low mass region.

Keywords: charmonium decays, light hadron spectroscopy

PACS numbers: 14.40.Pq, 13.25.-k, 13.25.Gv

1. $\psi(4040)/\psi(4160) \rightarrow \eta J/\psi$

Experimentally well established structures $\psi(4040)$, $\psi(4160)$, and $\psi(4415)$ resonances above the $D\bar{D}$ production threshold are of great interest but not well understood, even decades after their first observation.

BESIII accumulated a 478 pb^{-1} data sample at a center-of-mass (CMS) energy of $\sqrt{s} = 4.009 \text{ GeV}$. Using this data sample, the processes $e^+e^- \rightarrow \eta J/\psi$ and $\pi^0 J/\psi$ cross section are measured¹. In this analysis, the J/ψ is reconstructed through its decays into lepton pairs while η/π^0 is reconstructed in the $\gamma\gamma$ final state. After imposing all of some selection criteria, a clear J/ψ signal is observed in the $\mu^+\mu^-$ mode while indications of a peak around $3.1 \text{ GeV}/c^2$ also exist in the e^+e^- mode.

A significant η signal is observed in $M(\gamma\gamma)$ in both $J/\psi \rightarrow \mu^+\mu^-$ and $J/\psi \rightarrow e^+e^-$, as shown in Fig. 1. No significant π^0 signal is observed. The $M(\gamma\gamma)$ invariant mass distributions are fitted using an unbinned maximum likelihood method. For the η signal, the statistical significance is larger than 10σ while that for the π^0 signal is only 1.1σ . The Born cross section for $e^+e^- \rightarrow \eta J/\psi$ is measured to be $(32.1 \pm 2.8 \pm 1.3) \text{ pb}$, and the Born cross section is found to be less than 1.6 pb at the 90% confidence level (C.L.) for $e^+e^- \rightarrow \pi^0 J/\psi$.

Belle used 980 fb^{-1} data to study the process $e^+e^- \rightarrow \eta J/\psi$ via ISR². η is reconstructed in the $\gamma\gamma$ and $\pi^+\pi^-\pi^0$ final states. Due to the high background level from Bhabha scattering, the $J/\psi \rightarrow e^+e^-$ mode is not used in conjunction with the decay mode $\eta \rightarrow \gamma\gamma$.

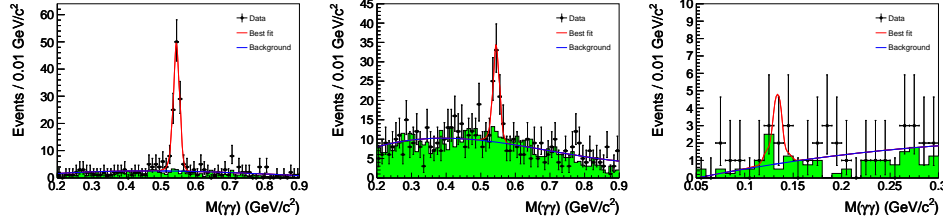
2 *Chengping Shen*

Fig. 1. Distributions of $M(\gamma\gamma)$ between 0.2 GeV/c^2 and 0.9 GeV/c^2 for $J/\psi \rightarrow \mu^+\mu^-$ (left panel) and for $J/\psi \rightarrow e^+e^-$ (middle panel) and distribution of $M(\gamma\gamma)$ below 0.3 GeV/c^2 for $J/\psi \rightarrow \mu^+\mu^-$ (right panel). Dots with error bars are data in J/ψ mass signal region, and the green shaded histograms are from normalized J/ψ mass sidebands. The curves show the total fit and the background term.

Clear η and J/ψ signals could be observed. A dilepton pair is considered as a J/ψ candidate if $M_{\ell^+\ell^-}$ is within $\pm 45 \text{ MeV}/c^2$ of the J/ψ nominal mass. The η signal region is defined as $M_{\pi^+\pi^-\pi^0} \in [0.5343, 0.5613] \text{ GeV}/c^2$ and $M_{\gamma\gamma} \in [0.5, 0.6] \text{ GeV}/c^2$. $-(\text{GeV}/c^2)^2 < M_{\text{rec}}^2 < 2.0 (\text{GeV}/c^2)^2$ is required to select ISR candidates, where M_{rec}^2 is the square of the mass recoiling against the $\eta J/\psi$ system. After event selections, an unbinned maximum likelihood fit is performed to the mass spectra $M_{\eta J/\psi} \in [3.8, 4.8] \text{ GeV}/c^2$ from the signal candidate events and η and J/ψ sideband events simultaneously, as shown in Fig. 2. The fit to the signal events includes two coherent P -wave Breit-Wigner functions, BW_1 for $\psi(4040)$ and BW_2 for $\psi(4160)$, and an incoherent second-order polynomial background. Statistical significance is 6.5σ for $\psi(4040)$ and 7.6σ for $\psi(4160)$. There are two solutions with equally good fit quality: $\mathcal{B}(\psi(4040) \rightarrow \eta J/\psi) \cdot \Gamma_{e^+e^-}^{\psi(4040)} = (4.8 \pm 0.9 \pm 1.4) \text{ eV}$ and $\mathcal{B}(\psi(4160) \rightarrow \eta J/\psi) \cdot \Gamma_{e^+e^-}^{\psi(4160)} = (4.0 \pm 0.8 \pm 1.4) \text{ eV}$ for one solution and $\mathcal{B}(\psi(4040) \rightarrow \eta J/\psi) \cdot \Gamma_{e^+e^-}^{\psi(4040)} = (11.2 \pm 1.3 \pm 1.9) \text{ eV}$ and $\mathcal{B}(\psi(4160) \rightarrow \eta J/\psi) \cdot \Gamma_{e^+e^-}^{\psi(4160)} = (13.8 \pm 1.3 \pm 2.0) \text{ eV}$ for the other solution, where the first errors are statistical and the second are systematic. The partial widths to $\eta J/\psi$ are found to be about 1 MeV.

2. Some results on η_c and $\eta_c(2S)$

The η_c mass and width have large uncertainties. The measured results of the η_c mass and width from J/ψ radiative transitions and two-photon fusion and B decays have large inconsistency. The most recent study by the CLEO-c experiment, using both $\psi(2S) \rightarrow \gamma\eta_c$ and $J/\psi \rightarrow \gamma\eta_c$, pointed out a distortion of the η_c line shape in $\psi(2S)$ decays.

With a $\psi(2S)$ data sample of 1.06×10^8 events, BESIII reported measurements of the η_c mass and width using the radiative transition $\psi(2S) \rightarrow \gamma\eta_c$ ³. Six modes are used to reconstruct the η_c : $K_S K^+ \pi^-$, $K^+ K^- \pi^0$, $\eta \pi^+ \pi^-$, $K_S K^+ \pi^+ \pi^- \pi^-$, $K^+ K^- \pi^+ \pi^- \pi^0$, and $3(\pi^+ \pi^-)$, where the K_S^0 is reconstructed in $\pi^+ \pi^-$, and the η and π^0 in $\gamma\gamma$ decays.

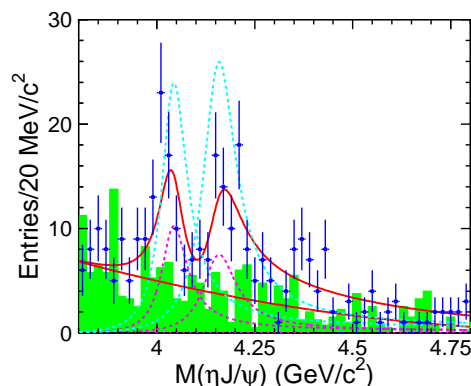


Fig. 2. The $\eta J/\psi$ invariant mass distribution and the fit results. The points with error bars show the data while the shaded histogram is the normalized η and J/ψ background from the sidebands. The curves show the best fit on signal candidate events and sideband events simultaneously and the contribution from each Breit-Wigner component. The dashed curves at each peak show the two solutions.

Figure 3 shows the η_c invariant mass distributions for selected η_c candidates, together with the estimated backgrounds. A clear η_c signal is evident in every decay mode. Assuming 100% interference between the η_c and the non-resonant amplitude, an unbinned simultaneous maximum likelihood fit was performed. In the fit, the η_c mass, width, and relative phases are free parameters, and the mass and width are constrained to be the same for all decay modes. Two solutions of relative phase are found for every decay mode, one represents constructive interference, the other for destructive. The measured mass is $M = 2984.3 \pm 0.6(stat.) \pm 0.6(syst.) \text{ MeV}/c^2$ and width $\Gamma = 32.0 \pm 1.2(stat.) \pm 1.0(syst.) \text{ MeV}$. The interference is significant, which indicates previous measurements of the η_c mass and width via radiative transitions may need to be rechecked. The results are consistent with that from photon-photon fusion and B decays; this may partly clarify the discrepancy puzzle.

Similarly the properties of the $\eta_c(2S)$ are not well-established either. The $\eta_c(2S)$ was first observed by the Belle collaboration in the process $B^\pm \rightarrow K^\pm \eta_c(2S)$, $\eta_c(2S) \rightarrow K_S^0 K^\pm \pi^\mp$. It was confirmed in the two-photon production of $K_S^0 K^\pm \pi^\mp$, and in the double-charmonium production process $e^+e^- \rightarrow J/\psi c\bar{c}$. Combining the world-average values with the most recent results from Belle and BaBar on two-photon fusion into hadronic final states other than $K_S^0 K^\pm \pi^\mp$, one obtains updated averages of the $\eta_c(2S)$ mass and width of $3637.7 \pm 1.3 \text{ MeV}/c^2$ and $10.4 \pm 4.2 \text{ MeV}$, respectively. $\eta_c(2S)$ was also observed in six-prong final states in two-proton processes including $3(\pi^+\pi^-)$, $K^+K^-2(\pi^+\pi^-)$, $2(K^+K^-)\pi^+\pi^-$, $K_S^0 K^\pm \pi^\mp \pi^+\pi^-$ by Belle collaboration. The measured averaged mass and width of $\eta_c(2S)$ are $3636.9 \pm 1.1 \pm 2.5 \pm 5.0 \text{ MeV}/c^2$ and $9.9 \pm 3.2 \pm 2.6 \pm 2.0 \text{ MeV}/c^2$. The results were reported in ICHEP2010 meeting, but the results are still preliminary up to date.

Recently BESIII collaboration searched for the M1 radiative transition $\psi(2S) \rightarrow$

4 Chengping Shen

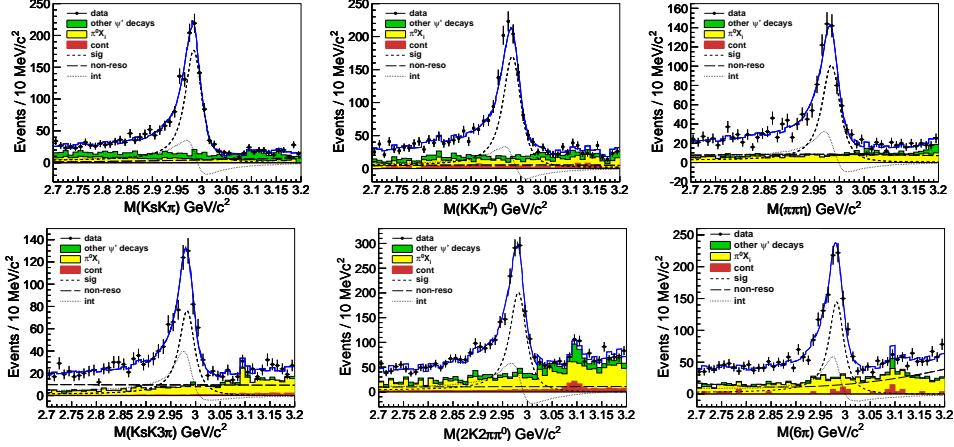


Fig. 3. The $M(X_i)$ invariant mass distributions for the decays $K_S K^+ \pi^-$, $K^+ K^- \pi^0$, $\eta \pi^+ \pi^-$, $K_S K^+ \pi^+ \pi^- \pi^-$, $K^+ K^- \pi^+ \pi^- \pi^0$ and $3(\pi^+ \pi^-)$, respectively, with the fit results (for the constructive solution) superimposed. Points are data and the various curves are the total fit results. Signals are shown as short-dashed lines; the non-resonant components as long-dashed lines; and the interference between them as dotted lines. Shaded histograms are (in red/yellow/green) for (continuum/ $\pi^0 X_i$ /other $\psi(2S)$ decays) backgrounds. The continuum backgrounds for $K_S K^+ \pi^-$ and $\eta \pi^+ \pi^-$ decays are negligible.

$\gamma \eta_c(2S)$ by reconstructing the exclusive $\eta_c(2S) \rightarrow K_S^0 K^\pm \pi^\mp \pi^+ \pi^-$ decay using $1.06 \times 10^8 \psi(2S)$ events ⁴.

The final mass spectrum of $K_S^0 K^\pm \pi^\mp \pi^+ \pi^-$ and the fitting results are shown in Fig. 4. The fitting function consists of the following components: $\eta_c(2S)$, χ_{cJ} ($J = 0, 1$, and 2) signals and $\psi(2S) \rightarrow K_S^0 K^\pm \pi^\mp \pi^+ \pi^-$, $\psi(2S) \rightarrow \pi^0 K_S^0 K^\pm \pi^\mp \pi^+ \pi^-$, ISR, and phase space backgrounds. The result for the yield of $\eta_c(2S)$ events is 57 ± 17 with a significance of 4.2σ . The measured mass of the $\eta_c(2S)$ is $3646.9 \pm 1.6(stat.) \pm 3.6(syst.)$ MeV/ c^2 , and the width is $9.9 \pm 4.8(stat.) \pm 2.9(syst.)$ MeV/ c^2 . The product branching fraction is measured to be $\mathcal{B}(\psi(2S) \rightarrow \gamma \eta_c(2S)) \times \mathcal{B}(\eta_c(2S) \rightarrow K_S^0 K^\pm \pi^\mp \pi^+ \pi^-) = (7.03 \pm 2.10(stat.) \pm 0.70(syst.)) \times 10^{-6}$. This measurement complements a previous BESIII measurement of $\psi(2S) \rightarrow \gamma \eta_c(2S)$ with $\eta_c(2S) \rightarrow K_S K^+ \pi^-$ and $K \bar{K} \pi$.

3. Evidence of the 1^3D_2 $c\bar{c}$ state ($X(3823)$)

During the last decade, a number of new charmonium ($c\bar{c}$)-like states were observed, many of which are candidates for exotic states. The observation of a D -wave $c\bar{c}$ meson and its decay modes would test phenomenological models. The undiscovered 1^3D_2 $c\bar{c}$ (ψ_2) and 1^3D_3 $c\bar{c}$ (ψ_3) states are expected to have significant branching fractions to $\chi_{c1}\gamma$ and $\chi_{c2}\gamma$, respectively. So Belle used $772 \times 10^6 B\bar{B}$ events to search for the possible structures in $\chi_{c1}\gamma$ and $\chi_{c2}\gamma$ mass spectra in the processes $B \rightarrow \chi_{c1}\gamma K$ and $B \rightarrow \chi_{c2}\gamma K$ decays, where the χ_{c1} and χ_{c2} decay to $J/\psi\gamma$ ⁵. The

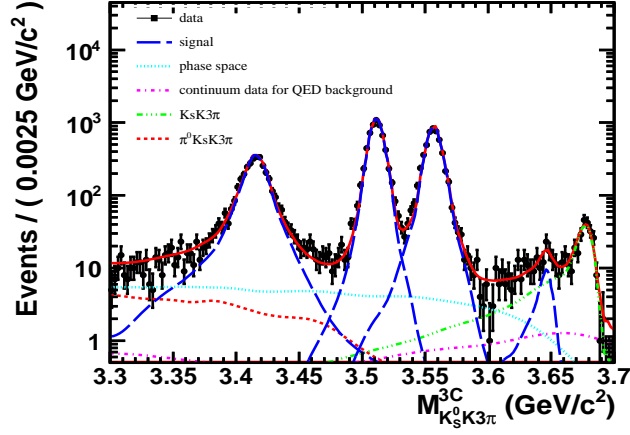


Fig. 4. The results of fitting the mass spectrum for χ_{cJ} and $\eta_c(2S)$. The black dots are the data, the blue long-dashed line shows the χ_{cJ} and $\eta_c(2S)$ signal shapes, the cyan dotted line represents the phase space contribution, the violet dash-dotted line shows the continuum data contribution, the green dash-double-dotted line shows the contribution of $\psi(2S) \rightarrow K_S^0 K^{\pm} \pi^{\mp} \pi^{\pm} \pi^{\mp}$, and the red dashed line is the contribution of $\psi(2S) \rightarrow \pi^0 K_S^0 K^{\pm} \pi^{\mp} \pi^{\pm} \pi^{\mp}$.

J/ψ meson is reconstructed via its decays to $\ell^+ \ell^-$ ($\ell = e$ or μ).

The $M_{\chi_{c1}\gamma}$ distribution from $B^{\pm} \rightarrow (\chi_{c1}\gamma)K^{\pm}$ and $B^0 \rightarrow (\chi_{c1}\gamma)K_S^0$ decays was shown in Fig. 5, where there is a significant narrow peak at 3823 MeV/ c^2 , denoted hereinafter as $X(3823)$. No signal of $X(3872) \rightarrow \chi_{c1}\gamma$ is seen. To extract the mass of the $X(3823)$, a simultaneous fit to $B^{\pm} \rightarrow (\chi_{c1}\gamma)K^{\pm}$ and $B^0 \rightarrow (\chi_{c1}\gamma)K_S^0$ is performed, assuming that $\mathcal{B}(B^{\pm} \rightarrow X(3823)K^{\pm})/\mathcal{B}(B^0 \rightarrow X(3823)K^0) = \mathcal{B}(B^{\pm} \rightarrow \psi'K^{\pm})/\mathcal{B}(B^0 \rightarrow \psi'K^0)$. The mass of the $X(3823)$ is measured to be $3823.1 \pm 1.8(stat.) \pm 0.7(syst.)$ MeV/ c^2 and signal significance is estimated to be 3.8σ with systematic uncertainties included. The measured branching fraction product $\mathcal{B}(B^{\pm} \rightarrow X(3823)K^{\pm})\mathcal{B}(X(3823) \rightarrow \chi_{c1}\gamma)$ is $(9.7 \pm 2.8 \pm 1.1) \times 10^{-6}$. No evidence is found for $X(3823) \rightarrow \chi_{c2}\gamma$. The properties of the $X(3823)$ are consistent with those expected for the ψ_2 (1^3D_2 $c\bar{c}$) state.

4. Search for $X(1835)$

In the radiative decay $J/\psi \rightarrow \gamma\pi^+\pi^-\eta'$, the BESII Collaboration observed a resonance, the $X(1835)$, with a statistical significance of 7.7σ . Recently the structure has been confirmed by BESIII in the same process with 2.25×10^8 J/ψ events.

Many theoretical models have been proposed to interpret its underlying structure. Some interpret $X(1835)$ as radial excitation of η' , a $p\bar{p}$ bound state, a glueball candidate, or a η_c -glueball mixture.

Belle first tried to search for the $X(1835)$ in the two-photon process $\gamma\gamma \rightarrow \eta'\pi^+\pi^-$ using a 673 fb^{-1} data sample with $\eta' \rightarrow \eta\pi^+\pi^-$, and $\eta \rightarrow \gamma\gamma$ ⁶.

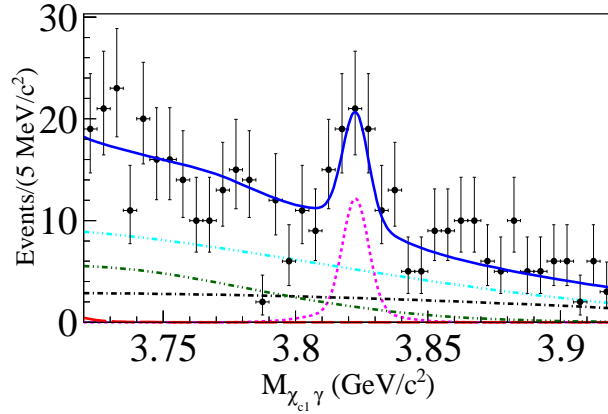


Fig. 5. Two-dimensional unbinned extended maximum likelihood fit projection of $M_{\chi_{c1}\gamma}$ distribution for the simultaneous fit of $B^\pm \rightarrow (\chi_{c1}\gamma)K^\pm$ and $B^0 \rightarrow (\chi_{c1}\gamma)K_S^0$ decays for $M_{bc} > 5.27$ GeV/c^2 .

Significant background reduction is achieved by applying a $|\sum \vec{p}_t^*|$ requirement ($|\sum \vec{p}_t^*| < 0.09$ GeV/c), which is determined by taking the absolute value of the vector sum of the transverse momenta of η' and the $\pi^+\pi^-$ tracks in the e^+e^- center-of-mass system. The $|\sum \vec{p}_t^*|$ distribution for the signal peaks at small values, while that for both backgrounds decreases toward $|\sum \vec{p}_t^*| = 0$ due to vanishing phase space.

The resulting $\eta'\pi^+\pi^-$ invariant mass distribution was shown in Fig. 6. According to existing observations, two resonances, $X(1835)$ and $\eta(1760)$, have been reported in the lower mass region above the $\eta'\pi^+\pi^-$ threshold. A fit with the $X(1835)$ and $\eta(1760)$ signals plus their interference is performed to the lower-mass events. Here, the $X(1835)$ mass and width are fixed at the BES value. There are two solutions with equally good fit quality; the results are shown in Fig. 6. In either solution, the statistical significance is 2.9σ for the $X(1835)$ and 4.1σ for the $\eta(1760)$. Upper limits on the product $\Gamma_{\gamma\gamma}\mathcal{B}(\eta'\pi^+\pi^-)$ for the $X(1835)$ at the 90% C.L. are determined to be 35.6 eV/c^2 and 83 eV/c^2 for the constructive- and destructive-interference solutions, respectively.

C-even glueballs can be studied in the process $e^+e^- \rightarrow \gamma^* \rightarrow H + \mathcal{G}_J$, where H denotes a $c\bar{c}$ quark pair or charmonium state and \mathcal{G}_J is a glueball. So if the $X(1835)$ was a candidate of glueball, it can also be searched for in the process $e^+e^- \rightarrow J/\psi X(1835)$ at $\sqrt{s} \approx 10.6$ GeV at Belle using a data sample of 672 fb^{-1} .

After all the event selections, the M_{recoil} distributions of the J/ψ are shown in Fig. 7. An unbinned simultaneous maximum likelihood fit to the M_{recoil} distributions was performed for the $\mu^+\mu^-$ and e^+e^- channels in the region of 0.8 $\text{GeV}/c^2 < M_{\text{recoil}} < 2.8$ GeV/c^2 , which constrains the expected signal from $J/\psi \rightarrow \mu^+\mu^-$ and $J/\psi \rightarrow e^+e^-$ to be consistent with the ratio of ε_i and \mathcal{B}_i , where ε_i and \mathcal{B}_i are the efficiency and branching fraction for the two channels, respectively. No significant

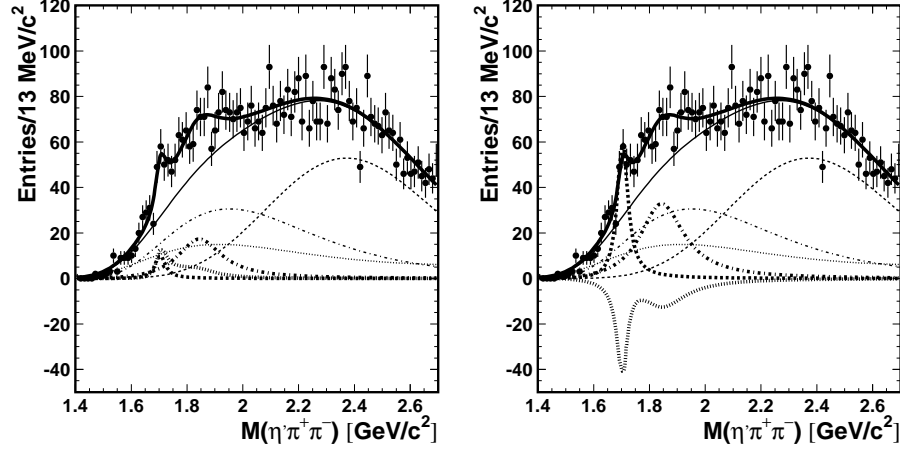


Fig. 6. Results of a combined fit for the $X(1835)$ and $\eta(1760)$ with interference between them. The points with error bars are data. The thick solid line is the fit; the thin solid line is the total background. The thick dashed (dot-dashed, dotted) line is the fitted signal for the $\eta(1760)$ ($X(1835)$, the interference term between them). The left (right) panel represents the solution with constructive (destructive) interference.

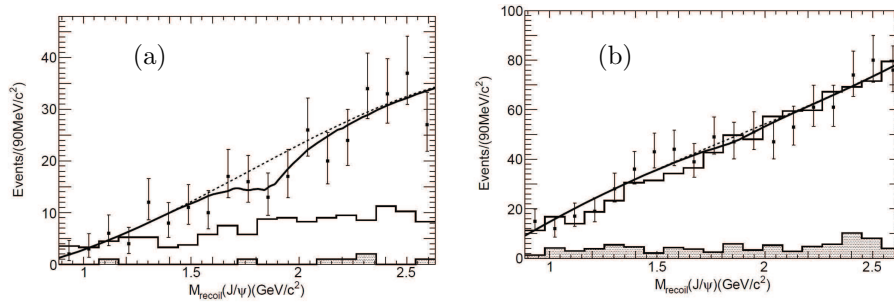


Fig. 7. The data points are for the distributions of the recoil mass against J/ψ reconstructed from (a) $\mu^+\mu^-$ and (b) e^+e^- . The histograms represent the backgrounds from the J/ψ sideband; the hatched histograms represent charmed- plus uds -quark backgrounds. The solid lines are results of the fits and the dashed lines are background shapes.

evidence of $X(1835)$ is found, and an upper limit is set on its cross section times the branching fraction: $\sigma_{\text{Born}}(e^+e^- \rightarrow J/\psi X(1835)) \cdot \mathcal{B}(X(1835) \rightarrow > 2 \text{ charged tracks}) < 1.3 \text{ fb}$ at 90% C.L. This upper limit is three orders of magnitude smaller than the cross section of prompt production of J/ψ . According to this work, no evidence was found to support the hypothesis of $X(1835)$ to be a glueball produced with J/ψ in the Belle experiment.

5. $\eta\eta$ mass spectra

According to lattice QCD predictions, the lowest mass glueball with $J^{PC} = 0^{++}$ is in the mass region from 1.5 to 1.7 GeV/ c^2 . However, the mixing of the pure glueball with nearby $q\bar{q}$ nonet mesons makes the identification of the glueballs difficult in both experiment and theory. Radiative J/ψ decay is a gluon-rich process and has long been regarded as one of the most promising hunting grounds for glueballs. In particular, for a J/ψ radiative decay to two pseudoscalar mesons, it offers a very clean laboratory to search for scalar and tensor glueballs because only intermediate states with $J^{PC} = \text{even}^{++}$ are possible.

Recently the study of $J/\psi \rightarrow \gamma\eta\eta$ was made by BESIII using 2.25×10^8 J/ψ events⁷, where the η meson is detected in its $\gamma\gamma$ decay. There are six resonances, $f_0(1500)$, $f_0(1710)$, $f_0(2100)$, $f_2'(1525)$, $f_2(1810)$, $f_2(2340)$, as well as 0^{++} phase space and $J/\psi \rightarrow \phi\eta$ included in the basic solution. The masses and widths of the resonances, branching ratios of J/ψ radiative decaying to X and the statistical significances are summarized in Table 1. The comparisons of the $\eta\eta$ invariant mass spectrum, $\cos\theta_\eta$, $\cos\theta_\gamma$ and ϕ_η distributions between the data and the partial wave analysis (PWA) fit projections are displayed in Fig. 8. The results show that the dominant 0^{++} and 2^{++} components are from the $f_0(1710)$, $f_0(2100)$, $f_0(1500)$, $f_2'(1525)$, $f_2(1810)$ and $f_2(2340)$.

Table 1. Summary of the PWA results, including the masses and widths for resonances, branching ratios of $J/\psi \rightarrow \gamma X$, as well as the significance. The first errors are statistical and the second ones are systematic. The statistic significances here are obtained according to the changes of the log likelihood.

Resonance	Mass(MeV/ c^2)	Width(MeV/ c^2)	$\mathcal{B}(J/\psi \rightarrow \gamma X \rightarrow \gamma\eta\eta)$	Significance
$f_0(1500)$	1468_{-15-74}^{+14+23}	$136_{-26-100}^{+41+28}$	$(1.65_{-0.31-1.40}^{+0.26+0.51}) \times 10^{-5}$	8.2σ
$f_0(1710)$	1759_{-25}^{+6+14}	172_{-16}^{+10+32}	$(2.35_{-0.11-0.74}^{+0.13+1.24}) \times 10^{-4}$	25.0σ
$f_0(2100)$	2081_{-36}^{+13+24}	273_{-24-23}^{+27+70}	$(1.13_{-0.10-0.28}^{+0.09+0.64}) \times 10^{-4}$	13.9σ
$f_2'(1525)$	1513_{-10}^{+5+4}	75_{-8}^{+12+16}	$(3.42_{-0.51-1.30}^{+0.43+1.37}) \times 10^{-5}$	11.0σ
$f_2(1810)$	1822_{-24-57}^{+29+66}	$229_{-42-155}^{+52+88}$	$(5.40_{-0.67-2.35}^{+0.60+3.42}) \times 10^{-5}$	6.4σ
$f_2(2340)$	$2362_{-30-63}^{+31+140}$	$334_{-54-100}^{+62+165}$	$(5.60_{-0.65-2.07}^{+0.62+2.37}) \times 10^{-5}$	7.6σ

$\eta\eta$ mass spectrum was also ever studied by Belle in two-photon process $\gamma\gamma \rightarrow \eta\eta$ using 393 fb⁻¹ data⁸. This pure neutral final states are selected with energy sum and cluster counting triggers, both of which information are provided by a CsI(Tl) electromagnetic calorimeter. The background was subtracted by studying sideband events in two-dimensional $M_1(\gamma\gamma)$ versus $M_2(\gamma\gamma)$ distributions. Further background effects are studied using $|\sum \vec{p}_t^*|$ distribution. Figure 9 shows the total cross sections. For the lower energy region $1.16 \text{ GeV} < W < 2.0 \text{ GeV}$, a PWA was performed to the differential cross section as shown in Fig. 10. In addition to the known $f_2(1270)$ and $f_2'(1525)$, a tensor meson $f_2(X)$ is needed to describe D_2 wave, which may correspond to $f_2(1810)$ state, and the mass, width and product of the two-photon decay width and branching fraction $\Gamma_{\gamma\gamma} \mathcal{B}(\eta\eta)$ for $f_2(X)$ are obtained to be 1737 ± 9

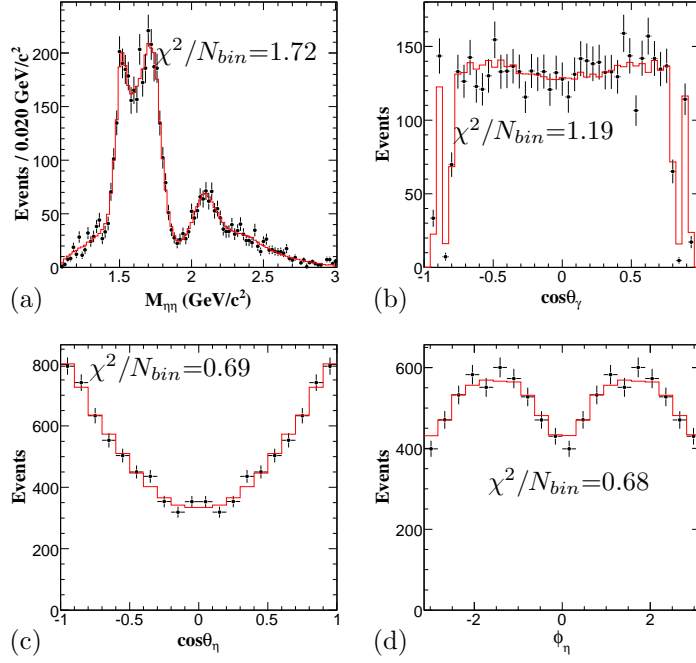


Fig. 8. Comparisons between data and PWA fit projections: (a) the invariant mass spectrum of $\eta\eta$, (b)-(c) the polar angle of the radiative photon in the J/ψ rest frame and η in the $\eta\eta$ helicity frame, and (d) the azimuthal angle of η in the $\eta\eta$ helicity frame. The black dots with error bars are data with background subtracted, and the solid histograms show the PWA projections. MeV/c^2 , 228^{+21}_{-20} MeV and $5.2^{+0.9}_{-0.8}$ eV, respectively.

6. $\omega\omega$, $\omega\phi$ and $\phi\phi$ mass spectra

An anomalous near-threshold enhancement, denoted as the $X(1810)$, in the $\omega\phi$ invariant-mass spectrum in the process $J/\psi \rightarrow \gamma\omega\phi$ was reported by the BESII experiment via PWA. The analysis indicated that the $X(1810)$ quantum number assignment favored $J^{PC} = 0^{++}$ over $J^{PC} = 0^{-+}$ or 2^{++} with a significance of more than 10σ . The mass and width are $M = 1812^{+19}_{-26}(\text{stat.}) \pm 18(\text{syst.}) \text{ MeV}/c^2$ and $\Gamma = 105 \pm 20(\text{stat.}) \pm 28(\text{syst.}) \text{ MeV}/c^2$, respectively, and the product branching fraction $\mathcal{B}(J/\psi \rightarrow \gamma X(1810)) \mathcal{B}(X(1810) \rightarrow \omega\phi) = [2.61 \pm 0.27(\text{stat.}) \pm 0.65(\text{syst.})] \times 10^{-4}$ was measured.

Possible interpretations for the $X(1810)$ include a tetraquark state, a hybrid, or a glueball state etc., a dynamical effect arising from intermediate meson rescattering, or a threshold cusp of an attracting resonance.

A PWA that uses a tensor covariant amplitude for the $J/\psi \rightarrow \gamma\omega\phi$ process was performed again in order to confirm the $X(1810)$ using $(225.3 \pm 2.8) \times 10^6 J/\psi$ events⁹. A PWA was performed on the selected $J/\psi \rightarrow \gamma\omega\phi$ candidate events to study the properties of the $\omega\phi$ mass threshold enhancement. In the PWA, the enhancement is denoted as X , and the decay processes are described with sequential

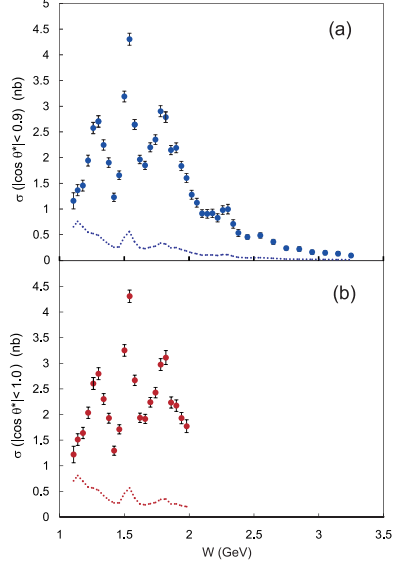
10 *Chengping Shen*

Fig. 9. (a) The cross section integrated over $|\cos \theta^*| < 0.9$ and (b) over $|\cos \theta^*| < 1.0$ for $W < 2.0$ GeV. Here θ^* is the angle of η in two-photon system. The dotted curve shows the size of the systematic uncertainty.

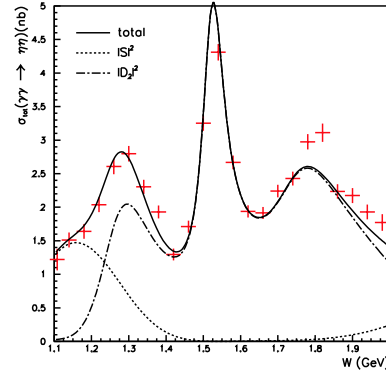


Fig. 10. Total cross sections and fitted curves for the nominal fit in the high mass region (solid curve). Dotted (dot-dashed) curves are $|S|^2$ ($|D_2|^2$) from the fit.

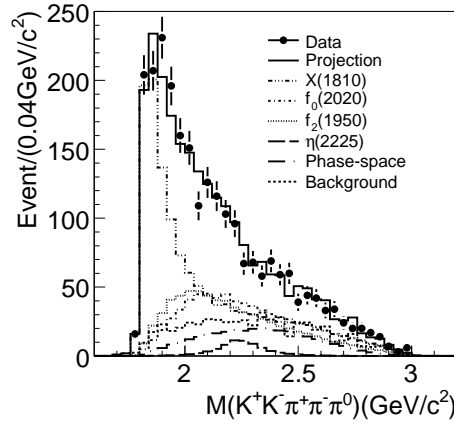


Fig. 11. The $K^+K^-\pi^+\pi^-\pi^0$ invariant-mass distribution between data and PWA fit projections.

2-body or 3-body decays: $J/\psi \rightarrow \gamma X$, $X \rightarrow \omega\phi$, $\omega \rightarrow \pi^+\pi^-\pi^0$ and $\phi \rightarrow K^+K^-$. The amplitudes of the 2-body or 3-body decays are constructed with a covariant tensor amplitude method. Finally, together with the contributions of the $X(1810)$ and phase-space, additional needed components are listed in Table 2 for the best

solution of the PWA fit. The $J^{PC} = 0^{++}$ assignment for the $X(1810)$ has by far the highest log likelihood value among the different J^{PC} hypotheses, and the statistical significance of the $X(1810)$ is more than 30σ . The mass and width of the $X(1810)$ are determined to be $M = 1795 \pm 7(stat.)_{-5}^{+13}(syst.) \pm 19(mod.)$ MeV/ c^2 and $\Gamma = 95 \pm 10(stat.)_{-34}^{+21}(syst.) \pm 75(mod.)$ MeV/ c^2 and the product branching fraction is measured to be $\mathcal{B}(J/\psi \rightarrow \gamma X(1810)) \times \mathcal{B}(X(1810) \rightarrow \omega\phi) = (2.00 \pm 0.08(stat.)_{-1.00}^{+0.45}(syst.) \pm 1.30(mod.)) \times 10^{-4}$. The contributions of each component of the best solution of the PWA fit are shown in Fig. 11. The enhancement is not compatible with being due either to the $X(1835)$ or the $X(p\bar{p})$, due to the different mass and spin-parity. The search for other possible states decaying to $\omega\phi$ would be interesting.

Table 2. Results from the best PWA fit solution.

Resonance	J^{PC}	$M(\text{MeV}/c^2)$	$\Gamma(\text{MeV}/c^2)$	Events	Significance
$X(1810)$	0^{++}	1795 ± 7	95 ± 10	1319 ± 52	$> 30\sigma$
$f_2(1950)$	2^{++}	1944	472	665 ± 40	20.4σ
$f_0(2020)$	0^{++}	1992	442	715 ± 45	13.9σ
$\eta(2225)$	0^{-+}	2226	185	70 ± 30	6.4σ
phase space	0^{-+}	—	—	319 ± 24	9.1σ

In the two-photon processes $\gamma\gamma \rightarrow \omega J/\psi$ and $\phi J/\psi$, a state $X(3915)$ and an evidence for $X(4350)$ were observed. It is very natural to extend the above theoretical picture to similar states coupling to $\omega\phi$, since the only difference between such states and the $X(3915)$ or $X(4350)$ is the replacement of the $c\bar{c}$ pair with a pair of light quarks. States coupling to $\omega\omega$ or $\phi\phi$ could also provide information on the classification of the low-lying states coupled to pairs of light vector mesons.

The $\gamma\gamma \rightarrow VV$ cross sections are shown in Fig. 12¹⁰. The fraction of cross sections for different J^P values as a function of $M(VV)$ is also shown in Fig. 12. We conclude that there are at least two different J^P components ($J = 0$ and $J = 2$) in each of the three final states. The inset also shows the distribution of the cross section on a semi-logarithmic scale, where, in the high energy region, we fit the $W_{\gamma\gamma}^{-n}$ dependence of the cross section.

We observe clear structures at $M(\omega\phi) \sim 2.2$ GeV/ c^2 , $M(\phi\phi) \sim 2.35$ GeV/ c^2 , and $M(\omega\omega) \sim 2.0$ GeV/ c^2 . While there are substantial spin-zero components in all three modes, there are also spin-two components near threshold.

7. Conclusion

I have reviewed some results on the charmonium and light hadron spectroscopy mainly from BESIII and Belle experiments, including the observation of $\psi(4040)/\psi(4160) \rightarrow \eta J/\psi$, some measurements on the $\eta_c/\eta_c(2S)$ resonance parameters and their decays, the evidence of the $\psi_2(1^3D_2)$ state in the $\chi_{c1}\gamma$ mass spectrum, the $X(1835)$ research in more processes, and the analysis of the $\eta\eta$, $\omega\phi$, $\phi\phi$ and $\omega\omega$ mass spectra.

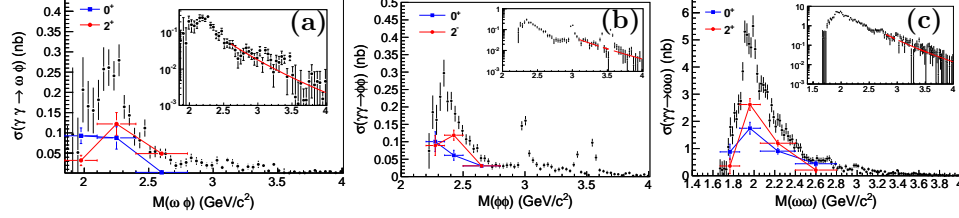
12 *Chengping Shen*

Fig. 12. The cross sections of $\gamma\gamma \rightarrow \omega\phi$ (a), $\phi\phi$ (b), and $\omega\omega$ (c) are shown as points with error bars. The fraction contributions for different J^P values as a function of $M(VV)$ are shown as the points and squares with error bars.

Acknowledgments

This work is supported partly by the Fundamental Research Funds for the Central Universities of China (303236).

References

1. BESIII Collab. (M. Ablikim *et al.*), *Phys. Rev. D* **86**, 071101(R) (2012).
2. Belle Collab. (X. L. Wang *et al.*), *Phys. Rev. D* **87**, 051101(R) (2012).
3. BESIII Collab. (M. Ablikim *et al.*), *Phys. Rev. Lett.* **108**, 222002 (2012).
4. BESIII Collab. (M. Ablikim *et al.*), *Phys. Rev. D* **87**, 052005 (2013).
5. Belle Collab. (V. Bhardwaj *et al.*), *Phys. Rev. Lett.* **111**, 032001 (2013).
6. Belle Collab. (C. C. Zhang *et al.*), *Phys. Rev. D* **86**, 052002 (2012).
7. BESIII Collab. (M. Ablikim *et al.*), *Phys. Rev. D* **87**, 092009 (2013).
8. Belle Collab. (S. Uehara *et al.*), *Phys. Rev. D* **82**, 114031 (2010).
9. BESIII Collab. (M. Ablikim *et al.*), *Phys. Rev. D* **87**, 032008 (2013).
10. Belle Collab. (Z. Q. Liu *et al.*), *Phys. Rev. Lett.* **108**, 232001 (2012).